Chapter 24

Quasars and Active Galactic Nuclei

Belinda J. Wilkes

24.1 INTRODUCTION

Quasars were discovered in the 1960s when two strong, compact radio sources in the third Cambridge radio survey, 3C273, 3C48, were identified with blue stellar objects [1–3]. Optical spectra revealed strong, broad, redshifted emission lines, suggesting the objects were at large distances and highly luminous. It was soon realized that the majority (~90%) are radio-quiet [4] and also that they are similar to the lower luminosity *active galactic nuclei* (AGN) discovered $\sim$ 20 years earlier [5]. This chapter includes definitions of many names and terms used for the various types of AGN, parameters used to characterize them, examples of optical spectra, etc. and many references to the literature. The aim is to provide a general reference and starting point for further study in many aspects of quasar research. A recent book [6] covers quasar research in more depth.

Quasars are generally believed to be small but highly luminous sources of radiation, probably powered by a supermassive ($\sim 10^{8-10}\mathcal{M}_\odot$) black hole, embedded in the center of a parent galaxy with the quasar's redshift indicating, via the expansion of the universe, its distance from our Galaxy. The radio-loud objects (see Table 24.1) also include two major components of radio emission: a compact core and extended lobes. These two components are thought to be linked by a relativistic, beamed jet originating in the core. Lower luminosity active galaxies include a mixture of objects, some of which are weaker versions of quasars and others of which are powered by star formation rather than a central black hole. The relationships between the various types remain a topic of some contention.

24.2 THE TYPES OF ACTIVE GALACTIC NUCLEI

The names and acronyms used for the many types or classes of active galaxies are listed in Table 24.1. Table 24.2 lists the properties of the main classes and Figures 24.1 and 24.2 show their distributions of relative radio–optical–X-ray luminosities and emission line ratios, respectively. Table 24.3 lists a few well-known objects from each of the major classes. Figure 24.3 shows the X-ray–infrared(IR) luminosity correlation for various classes of AGN and also normal galaxies.

Figures 24.4(a)–24.4(f) show optical/ultraviolet (UV) spectra of examples of the five classes: quasar (low and high redshift); BALQSO; BL Lac; Sy1; and NLXG.

Table 24.1. *Common names.*

General	Active galactic nucleus (AGN)	General term for an object containing nonstellar activity in its nucleus and [usually] optical/UV emission lines
	Quasar/QSO[a]	General terms for high-luminosity ($M < -23$) AGN with broad emission lines
	QSO	Quasi-stellar object
	BALQSO	Broad absorption line QSO
Radio	RQQ	Radio-quiet quasar, ${R_L}^b < 1.0$
	RLQ/QSRS	Radio-loud quasar, ${R_L}^b > 1.0$
	CDQ	Core-dominated, radio-loud quasar, $R^b > 1.0$
	LDQ	Lobe-dominated, radio-loud quasar, $R^b < 1.0$
	CSS	Core-dominated, steep spectrum RLQ
	GPS	Gigahertz peaked source, subset of CDQ with narrow (FWHM 1–2 decades) radio continua [1]
	FRI	Edge-darkened radio source, $L(1400\ \mathrm{MHz}) < 10^{25}\ \mathrm{W\,Hz^{-1}}$ (Fanaroff-Riley) [2]
	FRII	Edge-brightened radio source, $L(1400\ \mathrm{MHz}) > 10^{25}\ \mathrm{W\,Hz^{-1}}$
	Superluminal	Radio source containing motion where $v_{\mathrm{app}} > c$
Blazars	Blazar	General term for BL Lacs, OVVs, and HPQs
	BL Lac Object	Active nucleus but no emission lines

Table 24.1. *(Continued.)*

	RBL/LBL	Radio-selected/Low Frequency BL Lacs
	XBL/HBL	X-ray selected/High Frequency BL Lacs
	HPQ	Highly polarized quasar, $P \gtrsim 0.03$, generally CDQs
	LPQ	Low polarization quasar, $P \lesssim 0.03$ (normal QSO)
	OVV	Optically violent variable (subset of HPQ)
LLAGN[c]		Low luminosity AGN, $M > -23$ [3,4]
	Seyfert 1 (Sy1)	LLAGN with broad permitted and narrow forbidden emission lines [5]
	NLS1	Narrow line Sy1 galaxy, permitted lines $< 2000\ \mathrm{km\,s^{-1}}$ [6]
	Seyfert 2 (Sy2)	LLAGN with narrow permitted and forbidden emission lines [5]
	Seyfert 1.5–1.9	Similar to Sy1 but with progressively weaker broad lines
	BLRG	Broad line radio galaxy ("radio-loud Sy1")
	NLRG	Narrow line radio galaxy ("radio-loud Sy2")
	LINER	Low-ionization nuclear emission line region, present in $\sim 1/3$ of all bright galaxies [7]
	NLXG	Narrow line X-ray galaxy: X-ray strong, $L_x > 10^{41}$ erg^{-1}, Sy2 [8]
	Ultraluminous IR galaxy (ULIRG)	Ultraluminous in far-IR, shows starburst and AGN characteristics, $L_{\mathrm{FIR}} > 10^{12}\ L_\odot$ [9]
	Starburst	Galaxy containing strong starburst activity

Notes

[a]Historically *quasar* was used to indicate radio-loud objects; nowadays both terms are often used interchangeably to describe the whole class of luminous AGN.

[b]For parameter definitions please refer to Section 24.4.

[c]Note that the divisions between the various types of LLAGN (LINERS, starbursts, Sy2, NLXG) are not well defined.

References

1. O'Dea, C.P., Baum, S.A., & Stanghellini, C. 1991, ApJ, **380**, 66
2. Fanaroff, B.L. & Riley, J.M. 1974 MNRAS, **267**, 31P
3. Filippenko, A.V. 1992, ASP Conf. Proc. **31**, 253
4. Osterbrock, D.E. 1993, ApJ, **404**, 551
5. Khachikian, E.Y., & Weedman, D.W. 1974, ApJ, **192**, 581
6. Osterbrock, D.E., & Pogge, R. W. 1985 ApJ, **297**, 166
7. Heckman, T.M. 1980, A&A, **87**, 152
8. Stocke, J.S., Morris, S.L., Gioia, I.M., Maccacaro, T., Schild, R., Wolter, A., Fleming, T.A., & Henry, J.P. 1991, ApJS, **76**, 813
9. Sanders, D., Soifer, T.B., Elias, J.H., Madore, B.F., Matthews, K., Neugebauer, G., & Scoville, N.Z. 1988, ApJ, **325**, 74

Table 24.2. *Properties of various types of AGN.*

Class	Lines: Brd[a]	Lines: Nar[b]	RL[c] (%)	P^d (%)	$\log L_O{}^e$ ($\mathrm{erg\,s^{-1}}$)	$\log L_x$ ($\mathrm{erg\,s^{-1}}$)	Comments
Quasar	$\surd$	$\surd$	10	< 3	44^f–48	44–48	LPQ
BALQSO	$\surd$	$\surd$	0	$\surd^g$	44–48	44–48	
BL Lac Obj.	⋯	⋯	100	3-40	44–46	44–46	

Table 24.2. *(Continued.)*

Class	Lines Brd[a]	Nar[b]	RL[c] (%)	P^d (%)	$\log L_O$[e] (erg s^{-1})	$\log L_x$ (erg s^{-1})	Comments
HPQ	√	√	100	3-40	44–48	44–48	CDQ, γ-ray [1]
GPS	√	√	100	< 2	44–48	44–48	CDQ
Seyfert 1/BLRG	√	√	10	< 3	42–44[f]	43–45	
Seyfert 2/BLRG	P^h	√	10	0–20	41–43	41–43	[O III]>[O II]
LINER	···	√	···	···	40–44	40–42	[O III]<[O II]
Starburst	···	√	···	···	···	<41	[O III]<[O II]
NLXG	···	√	···	···	40–44	42–43.5	[O III]>[O II]

Notes

[a]Broad emission lines (FWHM~1000–10 000 km s^{-1}).

[b]Narrow emission lines (FWHM~100–1000 km s^{-1}).

[c]Rough percentage of radio-loud objects in the class.

[d]Typical percentage polarization in the optical continuum.

[e]Optical continuum luminosity not from stars.

[f]A dividing luminosity ($M_V \sim -23$; $L_O \sim 10^{44}$ erg^{-1}) between quasars and Sy1's is generally used [2].

[g]Frequently have high ($> 3\%$) polarization [3].

[h]Broad lines seen in polarized light for a subset [4].

References

1. Fichtel, C.E., *et al.* 1994, ApJS, **94**, 551
2. Schmidt, M., & Green, R.F. 1983, ApJ, **269**, 352
3. Glenn, J., Schmidt, G.D., & Foltz, C.B. 1994, ApJ, **434**, L47
4. Miller, J.S. 1994, in The Physics of Active Galaxies, eds. G.V. Bicknell, M.A. Dopita, & P.G. Quinn, ASP Conf. Ser. **54**, 149

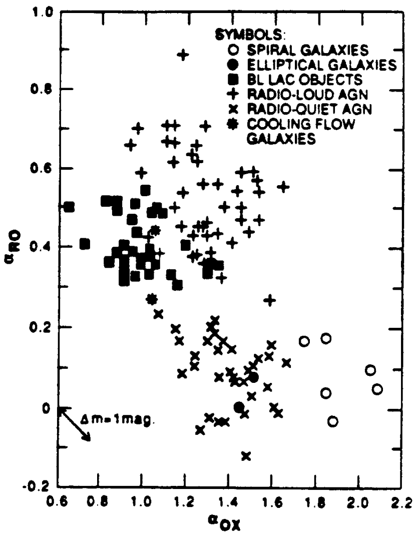

Figure 24.1. Relative radio–optical–X-ray properties of the several types of AGN and galaxies (from [7]). $\alpha_{\rm ro}$,$\alpha_{\rm ox}$ are the effective radio-optical and optical–X-ray slopes; see Sec. 24.4.

Table 24.3. *A selection of well-known objects of various types.*

Name	Class	α (2000)	δ (2000)	Redshift	V	Reference
3C273	RLQ	12 29 06.7	+02 03 09	0.158	13.02	[1]
3C48	RLQ	01 37 41.3	+33 09 35	0.367	16.06	[2]
S5 0014+81	RQQ	00 16 44.4	−04 04 11	3.384	16.5	[3]
NAB0205+024	RQQ	02 07 49.9	+02 42 56	0.155	15.39	[2]
PG1211+143	RQQ	12 14 17.6	+14 03 13	0.085	14.63	[3]
PC1247+3406	RQQ	12 49 42.1	+33 49 52	4.897	20.4	[3]
HS1946+7658	RQQ	19 44 55.0	+77 05 52	3.02	15.8	[3]
PHL5200	BALQSO	22 28 30.3	−05 18 55	1.981	17.7	[2]
1232+1325	BALQSO	12 34 58.3	+13 08 55	2.36	19.5	[4,3]
BL Lac	BL Lac	22 02 43.3	+42 16 40	0.0686	14.5	[2,5]
PKS2155−304	BL Lac	21 58 52	−30 13 29	0.116	14	[2,5]
3C446	OVV	22 25 47.3	−04 57 01	1.404	17.19	[2]
3C345	OVV	16 42 58.8	+39 48 37	0.595	15.96	[2]
3C279	OVV[a]	12 56 11.1	−05 47 22	0.538	17.75	[3]
I Zw 1	Sy1	00 53 34.9	+12 41 36	0.061	14.07	[2]
NGC5548	Sy1	14 17 59.6	+25 08 12	0.017	13.73	[3]
NGC4151	Sy1	12 10 32.5	+39 24 21	0.003	11.85	[3]
NGC4051	Sy1	12 03 09.6	+44 31 53	0.002	12.92	[3]
NGC1068	Sy2	02 42 40.7	−00 00 47	0.003	10.83	[3]
MRK 1	Sy2	01 16 07.2	+33 05 22	0.016	14.96	[3]
3C390.3	BLRG	18 42 08.9	+79 46 17	0.057	15.38	[3]
3C445	BLRG	22 23 49.7	−02 06 13	0.057	15.77	[3]
3C234	NLRG	10 01 49.5	+28 47 09	0.185	17.27	[3]
MRK 348	NLXG	00 48 47.2	+31 57 25	0.014	14.59	[3]
NGC1052	LINER	02 41 04.7	−08 15 21	0.005	12.31	[3]
NGC4258[b]	LINER	12 18 57.5	+47 18 14	0.002	11.65	[3]
PKS2322−12	LINER	23 25 19.7	−12 07 26	0.082	17.2	[3]
IF10214+4724	ULIRG[c]	10 24 34.6	+47 09 10	2.286	20.5	[5]
NGC7714	Starburst	23 36 14.1	+02 09 18	0.009	14.36	[6,3]
0833+652	Starburst	08 33 57.4	+65 17 46	0.057	13	[7]

Notes

[a] Strong γ-ray source. Hartmann *et al.* 1992, ApJ, **385**, L1

[b] A central, edge-on (i=83°) Keplerian disk revealed by water maser emission provides the first measured black hole mass in an AGN of 3.6×10^7 $\mathcal{M}_\odot$ [8].

[c] Ultraluminous infrared galaxy, gravitational lens [9].

References

1. Hewitt, A., & Burbidge, G. 1993, ApJS, **87**, 451
2. Hewitt, A., & Burbidge, G. 1989, ApJS, **69**, 1
3. Véron-Cetty, M.-P., & Veron, P. 1993, ESO Scientific Report No. 13
4. Weymann, R.J., Morris, S.L., Foltz, C.B., & Hewett, P.C. 1991, ApJ, **373**, 23
5. NASA/IPAC Extragalactic Database (NED); http://nedwww.ipac.caltech.edu
6. Weedman, D.W., Feldman, F.R., Balzano, V.A., Ramsey, L.W., Sramek, R.A., & Wu, C.-C. 1981, ApJ, **248**, 105
7. Margon, B., Anderson, S.F., Mateo, M., Fich, M., & Massey, P. 1988, ApJ, **334**, 597
8. Miyoshi, M., Moran, J., Herrnstein, J., Greenhill, L., Nakai, N., Diamond, P., & Inoue, M. 1995 Nature **373**, 127
9. Goldrich, R.W., Miller, J.S., Martel, A., Cohen, M.H., Tran, H.D. Ogle, P.M., & Vermeulen, R.C. 1996, ApJL, **456**, 9

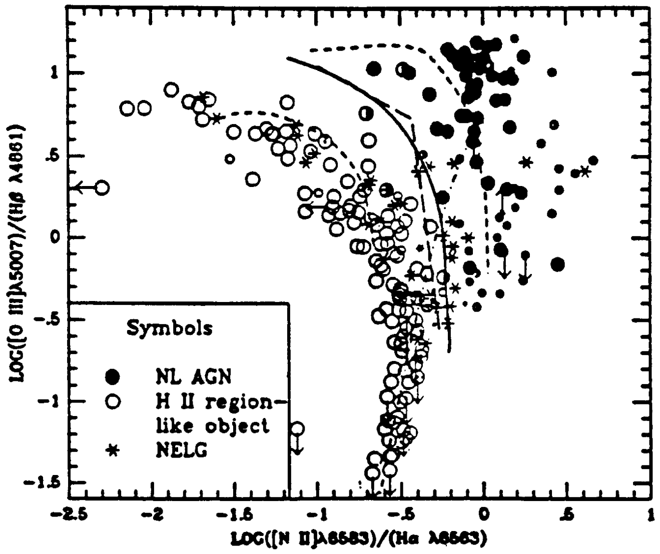

Figure 24.2. An example of a line ratio diagram showing the behavior of various types of LLAGN (from [8], their Fig. 1). Symbols are as shown with open symbols indicating H II and starburst objects. The solid curve divides AGNs from H II region–like objects. Four short-dashed lines are H II region models [9] for $T_* = 56\,000, 45\,000, 38\,500, 37\,000$ K top to bottom. Long dashed curve represents H II region models [10].

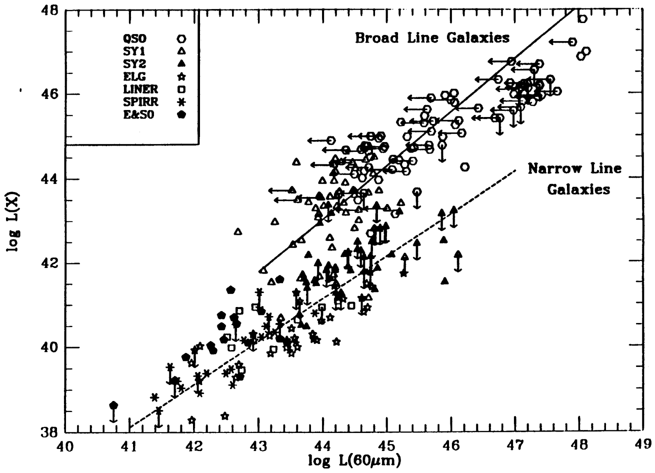

Figure 24.3. The correlation of X-ray and IR luminosities for broad- and narrow-lined objects (from [11]). SPIRR=spiral/irregular galaxy; E&SO=elliptical and SO galaxies; ELG=starburst or extragalactic H II region.

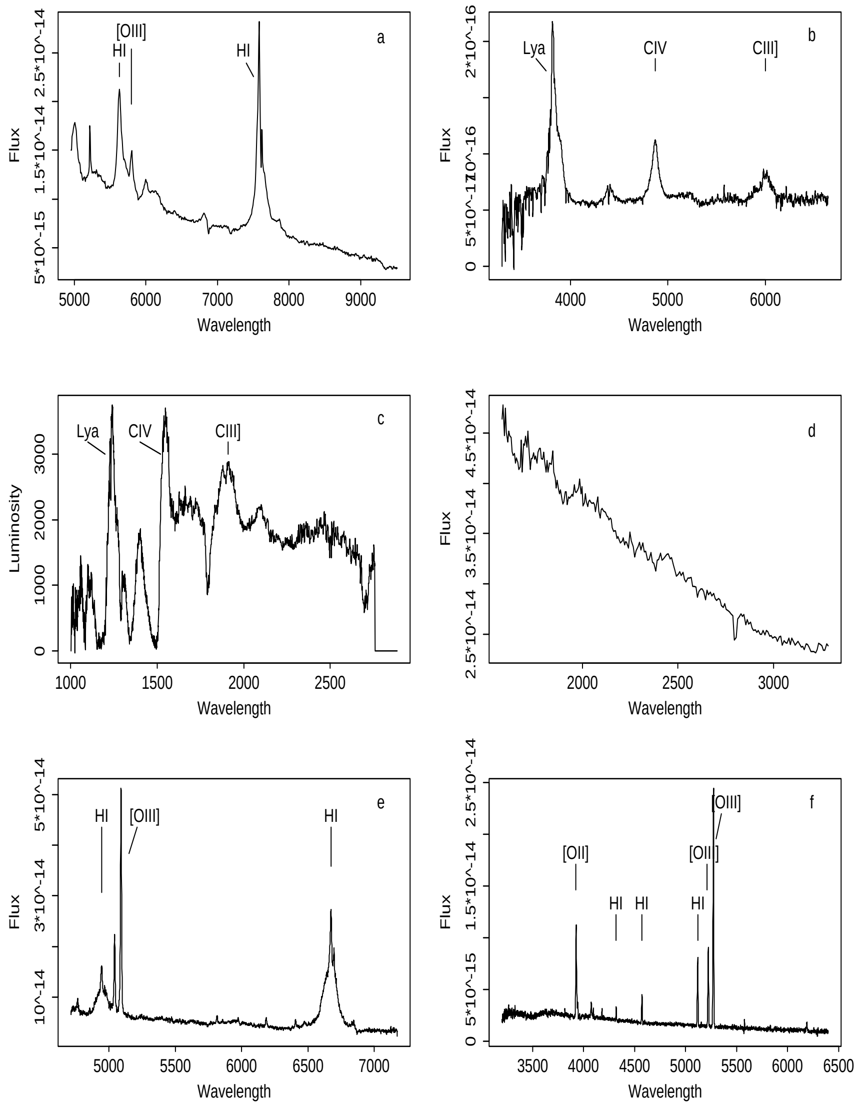

Figure 24.4. Optical/UV spectra of various types of quasar and active galaxy: (a) Optical spectrum of low-redshift quasar 3C273 ($z = 0.158$) observed with the 1.5-m telescope at CTIO, Feb 1989. (b) Optical spectrum of high-redshift quasar Q1101-264 ($z = 2.144$, [12, 13]). (c) Rest frame ultraviolet spectrum of the BALQSO 1232+1325 ($z = 2.364$) in units of erg s^{-1} Å^{-1}, courtesy of Craig Foltz [14]. (d) HST ultraviolet spectrum of the BL Lac PKS2155-305 in units of erg s^{-1} Å^{-1}, courtesy of Paul Smith [15]. (e) Optical spectrum of the Seyfert 1 galaxy NGC5548 ($z = 0.017$) generated by combining spectra between 13 and 19 April 1993 taken as part of the International AGN Watch monitoring campaign [16] on the SAO 60-in. telescope on Mt. Hopkins, Arizona. (f) Optical spectrum of the starburst galaxy PG0119+229 taken on 9 Jan 1989 with the SAO Multiple Mirror Telescope (MMT) on Mt. Hopkins, Arizona.

24.3 CATALOGS AND SURVEYS

In Table 24.4 a list of major optical surveys is given. Note that the number of quasars is a function of magnitude limit and thus numbers are only approximate. The total number of quasars generally reflects the number in the complete part of the survey. In cases where surveys are published in installments, the most recent/complete reference is given.

Table 24.4. *Major optical quasar surveys.*[a]

Name	$m_{\rm lim}$	$z_{\rm max}$	Area (deg^2)	n(QSOs)^b	Reference
BQS("PG")	~ 16	2.2	10^4	114	[1]
Edinburgh UVX	16.5	2.2	330	12	[2]
Hamburg	17.5	3.1	1000	160	[3]
MBQS	17.65	2.2	109	32	[4]
AB	18.25	2.2	35.5	22	[5]
HBQS	18.75	2.2	153	285	[6]
LBQS	18.85	3.4	454	1055	[7]
BF	19.8	2.2	1.72	35	[5]
SA94	19.9	2.2	10.0	94	[8]
CTIO 4m	~ 20	3.4	5.1	66	[9]
WHO	20 (R)	4.5	46	85	[10]
CFHT	20.5	3.4	9.40	268	[11]
SSG2	~ 20.5	4.5	7.84	8	[12]
Durham	21.0	2.2	11.9	397	[13]
SSG1	~ 22	4.5	0.91	10	[14]
(ZM)^{2}B	22.0	2.9	0.5	52	[15]
BJS	22.0	2.9	0.85	62	[16]
KOKR	22.6	3.2	0.29	30	[17]
DMS	23.8	4.36	0.83	55	[18]

Notes

[a] For a conference on Quasar surveys see [19].
[b] n is the number of QSOs in the survey.

References

1. Schmidt, M., & Green, R.F. 1983, ApJ, **269**, 352
2. Goldschmidt, P., Miller, L., LaFranca, F., & Christiani, S. 1992, MNRAS, **256**, 65P
3. Reimers, D., Koehler, T. & Wisotzki, L 1996 A&AS **115**, 235
4. Mitchell, K.J., Warnock, A., III, & Usher, P.D. 1984, ApJ, **68**, 449
5. Marshall, H.L., Avni, Y., Bracessi, A., Huchra, J.P., Tananbaum, H., Zamorani, G., & Zitelli, V. 1984, ApJ, **283**, 50
6. Cristiani, S. *et al.* 1995 A&AS, **112**, 347
7. Hewett, P.C., Foltz, C.B., & Chaffee, F.H., 1995, AJ, **109**, 1498
8. LaFranca, F., Cristiani, S., & Barbieri, C. 1992, AJ, **103**, 1062
9. Osmer, P.S. 1980, ApJS, **42**, 523
10. Warren, S.J., Hewett, P.C., & Osmer, P.S. 1991, ApJS, **76**, 23
11. Crampton, D., Cowley, A.P., & Hartwick, F.D.A. 1989, ApJ, **345**, 59
12. Schmidt, M., Schnneider, D.P., & Gunn, J.E. 1986, ApJ, **310**, 518
13. Boyle, B.J., Fong, R., Shanks, T., & Peterson, B.A. 1990, MNRAS, **241**, 1
14. Schmidt, M., Schnneider, D.P., & Gunn, J.E. 1986, ApJ, **306**, 411
15. Zitelli, V., Mignoli, M., Zamorani, G., Marano, B., & Boyle, B.J. 1992, MNRAS, **256**, 349
16. Boyle, B.J., Jones, L.R., Shanks, T., Marano, B., Zitelli, V., & Zamorani, G. 1991, in The Space Distribution of Quasars, APS Conf. Ser. **21**, 191
17. Koo, D.C., & Kron, R.G. 1988, ApJ, **325**, 92
18. Kennefick, J.D., Osmer, P.S., Hall, P.B. & Green, R.F. 1997, ApJ, **114**, 2269
19. Crampton, D. 1991, The Space Distribution of Quasars, ASP Conf. Ser. 21

24.3.1 Other Compilations and Surveys

General catalogs	Quasars	Hewitt & Burbidge [17]
	Quasars, BL Lacs, and Sy1s	Veron and Veron [18]
	BL Lacs	Padovani & Giommi [19]
	Emission line galaxies	Hewitt & Burbidge [20]
	Quasar absorption lines	Junkkarinen *et al.* [21]
Optical	Michigan Tololo QSO survey	MacAlpine, Lewis, & Smith [22]
	Optical spectra of PKS* AGN	Wilkes *et al.* [23]
	Anderson and Margon	Anderson & Margon [24]
	Parkes ±4 deg, optical	Baldwin, Wampler, & Gaskell [25]
	Liners	Keel [26]
	BALQSOs	Wolfe *et al.* [27]
	APM* High-Redshift Survey	Irwin, McMahon, & Hazard [28]
	PTGS*	Schneider, Schmidt & Gunn [29]
Ultraviolet	UV Spectra	Kinney *et al.* [30]
		Lanzetta *et al.* [31]
	AGN and galaxies	Kinney *et al.* [32]
	LLAGN	Ho *et al.* [33]
Infrared	IRAS PSC* AGN	Low *et al.* [34]
	IRAS: 12 micron	Rush, Malkan & Spinoglio [35]
	2MASS	Kleinmann *et al.* 1994 [36]
SED*	PG (Palomar Green)	Sanders *et al.* [37]
	Blazars	Impey & Neugebauer [38]
	Einstein quasars	Elvis *et al.* [39]
X-ray	EMSS (Extended Medium Sensitivity Survey)	Maccacaro *et al.* [40]
	HEAO 1 A-2 High Latitude	Piccinotti *et al.* [41]
	HEAO 1 MC-LASS*	Schwartz *et al.* [42]
	Einstein X-ray Quasar Database	Wilkes *et al.* [43]
	Einstein Slew Survey	Elvis *et al.* [44]
	EXOSAT High Galactic Latitude	Giommi *et al.* [45]
	ROSAT All Sky Survey: BSC*	Voges *et al.* [46]
	ROSAT/AAT QSO Survey	Boyle *et al.* [47]
	RASS/LBQS	Green *et al.* [48]
	CCRSS	Boyle *et al.* [49]
	RIXOS	Puchnarewicz *et al.* [50]
	WGACAT	Singh *et al.*[51]
γ-ray	1st EGRET Catalogue	Fichtel *et al.* [52]
Radio	PKS* ±4-deg quasar sample	Masson & Wall [53]
	PG	Kellerman *et al.* [54]
	1-Jy sample	Kuhr *et al.* [55]
	NVSS	Condon *et al.* [56]
	FIRST	Gregg *et al.* [57]

* PKS: Parkes, APM: Automated Plate Measuring Machine, PTGS: Palomar Transit Grism Survey, PSC: Point Source Catalogue, SED: spectral energy distribution, MC-LASS: Modulation Collimator-Large Area Sky Survey, BSC: Bright Source Catalogue.

24.4 COMMONLY MEASURED PARAMETERS

The following list gives some of parameters commonly used (or used here) in characterizing quasars and active galaxies and Table 24.5 gives the range of these parameters (where appropriate) for the various types of AGN.

Redshift,z = $(1+z) = \frac{\lambda_{\rm obs}}{\lambda_{\rm rest}} = \frac{\nu_{\rm rest}}{\nu_{\rm obs}}$ where $\lambda_{\rm obs}$, $\lambda_{\rm rest}$ =observed, rest wavelengths and $\nu_{\rm obs}$, $\nu_{\rm rest}$ = observed, rest frequency

L_x = Luminosity at 2 keV (rest frame) in erg s^{-1} Hz^{-1}

$L_{\rm opt}$ = Luminosity at 2500 Å (rest frame) in erg s^{-1} Hz^{-1}

α = Spectral index: $F_\nu \propto \nu^\alpha$ (N.B. negative α commonly used in x and γ-rays)

Γ = Photon index: $-(\alpha+1)$ (used in X-rays)

$\alpha_{\rm ox}$ = Effective optical to X-ray slope [58]

$$\alpha_{\rm ox} = -\frac{\log \frac{L_x}{L_{\rm opt}}}{\log \frac{\nu_x}{\nu_{\rm opt}}}$$

ν_x corresponding to 2 keV; $\nu_{\rm opt}$ corresponding to 2500 Å; ratio = 2.605

$\alpha_{\rm ro}$ = Effective radio to optical slope (5 GHz and either 2500 Å [59] or V [60])

ν_c = Critical/turnover frequency, generally in far-IR/radio band

W_λ, EW = Rest frame equivalent width: $W_\lambda({\rm rest}) = \frac{W_\lambda({\rm obs})}{1+z}$

FWHM = Full width at half maximum intensity for a spectral line

Lyman edge = Relative change of the continuum level at the Lyman limit, 912 Å

R_L = Core radio loudness: $\log(F_R({\rm core})/F_B)$ [61]

R_{L_t} = Total radio loudness: $\log(F_R({\rm total})/F_B)$ [62]

R or R(θ) = radio core dominance: $\log\left(\frac{\text{flux density of beamed component}}{\text{flux density of unbeamed components}}\right)$ (5 GHz, rest frame) [63], where θ is the angle between the line of sight and the direction of approach of the lobes

R_T = $R(\theta = 90^\circ)$ [63]

$C_{\rm UV/IR}$ = Blue bump strength: $\frac{L(0.1-0.2\ \mu{\rm m})}{L(1-2\ \mu{\rm m})}$ [64]

l = Compactness parameter, $\frac{\sigma_T L}{m_e c^3 R}$ [65], where L =luminosity (in region of variability data), m_e= electron mass, R =size of source (from variability), σ_T = Thompson cross section, c =velocity of light

U = Ionization parameter, $\frac{\int_{\nu_L}^{\infty} L_\nu \frac{d\nu}{h\nu}}{4\pi r^2 c n_e}$ [66] where ν_L = frequency at Lyman limit, n_e = electron density, r = distance from source

$\mathcal{M}_{\rm BH}$ = Derived mass of central black hole

$\dot{\mathcal{M}}$ = Accretion rate

P = Percentage polarization

θ_p = Position angle of polarization

Δm = Amplitude of variation in magnitudes

T_{var} = Variability time scale, e.g., doubling time

γ = Lorentz factor, $=\sqrt{(1-\beta^2)} = E/mc^2$ where $\beta = v/c$

μ = Angular velocity (mas yr^{-1}, mas=milliarcseconds, used to measure superluminal knots)

$\beta_{\rm app}$ = v/c where v =apparent linear velocity in the sky plane

$$\frac{[\text{O III}]}{\text{H}\beta} = \frac{[\text{O III}]\lambda 5007 + \lambda 4959}{\text{H}\beta}$$

$$\frac{[\text{N II}]}{\text{H}\alpha} = \frac{[\text{N II}]\lambda 6583}{\text{H}\alpha}$$

$$\frac{[\text{O I}]}{\text{H}\alpha} = \frac{[\text{O I}]\lambda 6300}{\text{H}\alpha}$$

$$\frac{[\mathrm{S\,II}]}{\mathrm{H}\alpha} = \frac{[\mathrm{S\,II}]\lambda6713 + \lambda6731}{\mathrm{H}\alpha}$$

$$\frac{[\mathrm{O\,II}]}{[\mathrm{O\,III}]} = \frac{[\mathrm{O\,II}]\lambda3727}{[\mathrm{O\,III}]\lambda5007}$$

$$\frac{[\mathrm{O\,I}]}{[\mathrm{O\,III}]} = \frac{[\mathrm{O\,I}]\lambda6300}{[\mathrm{O\,III}]\lambda5007}$$

ΔE = $1/3[\Delta E(\lambda5007/\lambda4861) + \Delta E(\lambda6844/\lambda6563) + \Delta E(\lambda6300/\lambda6563)]$ average excess of these ratios above that of an H II region [67]

Table 24.5. *Range of values for some common parameters.*

	RQQ	CDQ	LDQ	Reference
z	0.1–4.9	0.1–4.3	0.1–4	
$\alpha_{\rm ox}$	1–2	1–1.6	1–1.6	[1,2]
α_X(0.1–3.5 keV)	0.5 to −2	−0 to −1	−0 to −1	[3]
α_X(2–10 keV)	−0.9 to −1.2	−0.5 to −0.9	−0.5 to −0.9	[4][a]
α_γ	0.9 ± 0.05^b	0.7–1.6	…	[5,6]
α_R	−0.2 to −1.0	$< 0.5^c$	> 0.5	[7,8]
α_O	−1.5 to 1	−1.5 to 1	−1.5 to 1	[9]
$\overline{\alpha}_{IR}$	−1.7	−1.7	−1.7	[10]
α_c	3.75 ± 0.48	1	1	[11,12]
R_L	< 1	> 1	> 1	[3]
R_{L_t}	< 1	> 1	> 1	[13]
$R(\theta)$	~ 0.6	> 1	< 1	[8]
$C_{\rm UV/IR}{}^d$	4.9±2.1	5.6±4.7	5.6±4.7	[14]
l	0 to >230	0 to >300	0 to >200	[15,16]
$P_{\rm opt}$	< 3	0–20	0–10	
FWHM (BLR)^e	$(1–7)\times10^3$	$(1–5)\times10^3$	$(1–10)\times10^3$	[17]
FWHM (NLR)^e	$(1–10)\times10^2$	$(1–10)\times10^2$	$(1–10)\times10^2$	
W_λ(Fe II)^f	0–120	0–50	0–70	[18]
$\log(\mathcal{M}_{\rm BH}/\mathcal{M}_\odot)^g$	8–10	8–10	8–10	[19]

Notes

[a]90% confidence range.
[b] High energy cutoff generally occurs $\gtrsim$ 100 keV
[c]Except for steep spectrum, core-dominated sources.
[d]Error is the dispersion in the distribution; CDQs and LDQs not distinguished due to small numbers of objects.
[e]in km s^{-1}
[f]$\lambda\lambda$ 4434–4684 Å.
[g]Model dependent.

References

1. Tananbaum, H. *et al.* 1979, ApJ, **234**, L9
2. Wilkes, B.J., Tananbaum, H., Worrall, D.M., Avni, Y., Oey, M.S., & Flanagan, J. 1994, ApJS, **92**, 53
3. Wilkes, B.J., & Elvis, M. 1987, ApJ, **323**, 243
4. Williams, O.R. *et al.* 1992, ApJ, **360**, 396
5. Fichtel, C.E. *et al.* 1994, ApJS, **94**, 551
6. Gondek, D., Zdziarski, A.A., Johnson, w.N., George, I.M., McNaron-Brown, K., Magdziarz, P., Smith, D. & Gruber, D. 1996 MNRAS, **282**, 646
7. Laing, P.A., & Peacock, J.A. 1980, MNRAS, **190**, 903
8. Kukula, M. J., Dunlop, J. S., Hughes, D. H., & Rawlings, S. 1998, MNRAS, in press
9. Francis, P.J., Hewett, P.C., Foltz, C.B., Chaffee, F.H., Weymann, R.J., & Morris, S.L. 1991, ApJ, **373**, 465

10. Berriman, G. 1990, ApJ, **354**, 148
11. Hughes, D.H., Robson, E.I., Dunlop, J.S., & Gear, W.K. 1993, MNRAS, **263**. 607
12. Peacock, J.A., & Wall, J.V. 1981, MNRAS, **194**, 331
13. Shastri, P., Wilkes, B.J., Elvis, M., & McDowell, J.C. 1993, ApJ, **410**, 29
14. McDowell, J.C., Elvis, M., Wilkes, B.J., Willner, S.P., Oey, M.S., Polomski, E., Bechtold, J., & Green, R.F. 1989, ApJ, **345**, L13
15. Done, C., & Fabian, A.C. 1989, MNRAS, **240**, 81
16. Lightman, A.P., & Zdziarski, A.A. 1987, ApJ, **319**, 643
17. Heckman, T.M. 1980, A&A, **87**, 152
18. Boroson, T., & Green, R. F. 1992, ApJS, **80**, 109
19. Sun, W.-S., & Malkan, M. 1989, ApJ, **346**, 68

24.5 EMISSION LINES

The presence of strong emission lines is the most definitive indication of activity in galactic nuclei. A recent conference procedings on this topic is [68] and includes several review articles. An older but very useful review can be found in [66]. Table 24.6 contains a list of multiplet wavelengths for UV–IR observed/candidate emission line features in quasar and Seyfert 1 galaxy spectra. A mean wavelength, assuming optically thin gas, is also given for convenience. For detailed atomic data on the individual lines refer to Chap. 4 and for X-ray features to Chap. 9. Little attempt has been made to include Iron (Fe) features, for comprehensive discussions of optical and ultraviolet Fe emission in quasars and AGN see [69, 70] and references therein. Figure 24.5 shows a composite UV/optical spectrum with the prominent features labeled.

The study of X-ray emission lines is a new and exciting one which the launch of AXAF in late 1998 promises to open up dramatically. Current studies of broad Fe Kα (6.4 keV) with Ginga and ASCA [71, 72] provide some of the best evidence to date for an accretion disk surrounding a central, supermassive black hole. A comprehensive review of X-ray emission from quasars is provided by [73] and a discussion of X-ray emission lines in AGN in [74].

Table 24.6. *IR–UV emission line features commonly observed in AGN.*

Element	Mean $\lambda^{a,b}$ (Å)	Component λ's^b (Å)	Reference	Ratio^c to Lyα
S VI	937.06		[1]	
Lyγ	972.54		[1]	
C III	977.02		[1]	
N III	990.98	989.80, 991.51, 991.58	[1]	
Lyβ	1025.72		[1]	
O VI	1033.82	1031.93, 1037.62	[1]	9.3
He II	1084.94		[2]	
Si II	1194.10	1197.39, 1194.50, 1193.29, 1190.42	[1]	
Lα	1215.67		[1]	
O V	1218.34		[1]	100
N V	1240.15	1238.82, 1242.80	[1]	
Si II	1263.31	1260.42, 1264.74, 1265.00	[1]	
O I	1303.49	1302.17, 1304.86, 1306.03	[1]	3.5
Si II	1307.64	1304.37, 1309.28	[1]	
C II	1335.31	1334.53, 1335.66, 1335.71	[1]	2.5
Si IV	1396.75	1393.76, 1402.77	[1]	19
O IV]	1402.34	1397.23, 1399.78, 1401.16, 1404.81, 1407.38	[1]	
N IV]	1486.50		[1]	
Si II	1531.18	1526.71, 1533.43	[1]	
C IV	1549.05	1548.20, 1550.77	[1]	63

Table 24.6. *(Continued.)*

Element	Mean $\lambda^{a,b}$ (Å)	Component λ's^{b} (Å)	Reference to Lyα	Ratio^{c}
He II	1640.42	1640.34, 1640.47	[2]	8
O III]	1664.15	1660.81, 1666.15	[1]	
Al II	1670.79		[1]	
N III]	1750.46	1746.82, 1748.65, 1749.67, 1752.16, 1754.00	[1]	
Si II	1813.98	1808.01, 1816.93, 1817.45	[1]	
Al III	1857.40	1854.72, 1862.79	[1]	
Si III]	1892.03		[1]	
C III]	1908.73		[1]	29
N II]	2141.36	2139.01, 2142.77	[1]	0.34
C II]	2326.58	2324.21, 2325.40, 2326.11, 2327.65, 2328.84	[1]	6.0
[Ne IV]	2418.70	2418.2, 2420.9	[3]	2.2
Mg II	2797.92	2795.53, 2802.71	[1]	34
He II	3203.07	3202.96, 3203.15	[2]	
[Ne V]	3345.83		[3]	0.52
[Ne V]	3425.87		[3]	1.0
[O II]	3726.67	3726.03, 3728.82	[3]	0.78
[Ne III]	3868.75		[3]	3.6
He I	3888.65		[4]	
[Ne III]	3967.47		[3]	1.3
Hϵ	3970.07		[4]	
[S II]	4068.60		[3]	
[S II]	4076.35		[3]	2.8
Hδ	4101.73		[4]	
Hγ	4340.46		[4]	13
[O III]	4363.21		[3]	
He II	4685.65	4685.4, 4685.7	[2]	
[Ar IV]	4711.34		[3]	
[Ar IV]	4740.20		[3]	
Hβ	4861.32		[4]	22
[O III]	4958.91		[3]	0.93
[O III]	5006.84		[3]	3.4
[N I]	5199.82^{d}		[4]	
[Ca V]	5309.18		[5]	
[Fe VII]	5721.11		[6]	
[N II]	5754.57		[3]	
He I	5875.7		[4]	
[Fe VII]	6086.92		[6]	
[O I]	6300.30		[3]	
[O I]	6363.78		[3]	
[Fe X]	6374.53		[3]	
Hα	6562.80		[4]	
[N II]	6548.06		[3]	
[N II]	6583.39		[3]	
[S II]	6716.47		[3]	
[S II]	6730.85		[3]	
O I	8446.5		[4]	
[S III]	9068.9		[3]	
He I	10830.20	10829.09, 10830.25, 10830.34	[4]	
Pα	18751.0		[4]	
Pβ	12818.1		[4]	

Notes

[a]Mean wavelength assuming optically thin gas, see Chap. 4.

[b]In vacuo for $\lambda < 2000$ Å, in air $\lambda > 2000$ Å.

[c]Mean ratio for prominent lines [$\gtrsim 0.5\%$ F(Lyα/NV) blend] based on the composite spectrum of [7].

[d]Reader & Corliss, [2], give 5197.94 Å.

References

1. Morton, D.C. 1991, ApJS, **77**, 119
2. Reader, J., & Corliss, C.H. 1980, NIST Spectroscopic Properties of Atoms and Atomic Ions Wavelengths, NSRDS-NBS Vol. 68, Part I
3. Kaufman, V., & Sugar, J.J. 1986, Phys. Chem. Ref. Data, **15**, 321
4. Weise, W.L. Smith, M.W. & Glennon, B.M. 1966, Atomic Transition Probabilities, Vol. 1 (National Bureau of Standards, Washington)
5. Weise, W.L. Smith, M.W. & Miles, B.M. 1969, Atomic Transition Probabilities, Vol. 2 (National Bureau of Standards, Washington)
6. Bowen, I.S. 1960, ApJ, **132**, 1
7. Francis, P.J., Hewett, P.C., Foltz, C.B., Chaffee, F.H., Weymann, R.J., & Morris, S.L. 1991, ApJ, **373**, 465

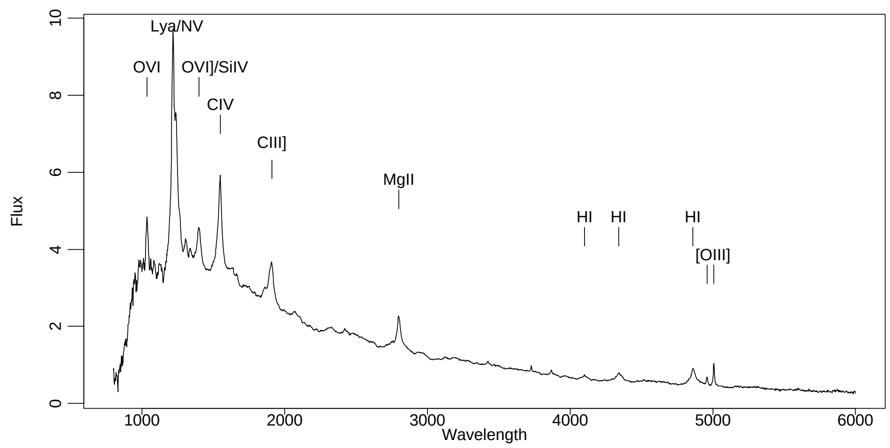

Figure 24.5. Composite optical/UV spectrum of a quasar [75].

24.5.1 The Broad Emission Line Region (BLR, BELR)

The broad emission lines that characterize the optical/UV spectra of quasars are thought to originate in gas photoionized by the central continuum source. The smooth profiles and large line widths lead to a popular scenario of large numbers of small clouds moving at high velocity. However the direction of this motion has not been generally determined. For a detailed summary of our knowledge of the BELR see [76]. Table 24.7 lists the physical parameters of the broad line region and the observational evidence that leads to these numbers. Reverberation mapping studies over the past $\sim$ 10 years have revolutionised these studies by providing a direct measure of the size of the emitting region in a few objects, eg. NGC5548 [77–79].

Table 24.7. *Parameters of the BLR.*

Parameter	Typical values	Based on
Electron density n_e	10^{8-12} cm^{-3}	[O III] λ5007, No; C III]λ1909, Yes[a]
Ionization parameter	$\log U \sim -1$	Line strengths + photoionization models
Temperature	10^4 K	Photoionization models
Size	0.01–0.1 pc	Variability studies in Sy1's [1]
	1 pc	in quasars
Cloud velocities	$10^3 - 10^4$ km s^{-1}	Observed linewidths
Covering factor	0.1	Observations of Lyman limit absorption
		photoionization models
N(H I)	$> 10^{22}$ cm^{-2}	Mg II, Fe II: yes
τ (Lyα)	10^8	Photoionization models

Notes
[a]But see [2].

References
1. Netzer, H. & Peterson, B.M. 1997, in Astronomical Time Series, ed. D. Maoz, A Sternberg & E. Leibowitz (Dordrecht: Kluwer), P.85
2. Mathur, S., Elvis, M.S. & Wilkes, B.J. 1995, ApJ, **452**, 230

24.5.2 The Narrow Emission Line Region (NLR, NELR)

Narrow emission lines are present in all varieties of AGN. They also originate mostly in photoionized gas, although collisionally ionized gas often contributes significantly. The gas is further from the continuum source than the BLR and thus has lower ionization and lower velocities. The density is also lower and many forbidden lines are present. Table 24.8 lists the physical parameters of the narrow line region and the observational evidence that leads to these numbers.

Table 24.8. *Parameters of the NLR.*

Parameter	Typical values	Based on
Electron density n_e	$\sim 10^{3-6}$ cm^{-3}	[O III] λ5007: yes
Ionization parameter	$\log U \sim -2$	Line strengths [1]
Temperature	10^4 K	Emission lines
Size	100 pc–>1 kpc	Photoionization models
$\log(\mathcal{M}/\mathcal{M}_\odot)$	-6	Emission lines
Cloud velocities	100–1000 km s^{-1}	Observed linewidths
N(H I)	> N(H I) for BLR	Photoionization models

Reference
1. Netzer, H. 1990, in Active Galactic Nuclei, eds. T. J.-L. Courvoisier and M. Mayor (Springer, Berlin), p. 57

24.5.3 Effects of Lines on Optical Magnitudes

The presence of emission lines within the bandpass of a given filter contribute significantly to the observed magnitudes of an AGN. Since this effect is a strong function of redshift, it is often useful to correct for the presence of the lines thus yielding magnitudes based on the continuum emission of the AGN alone. The correction, based on the line equivalent width, can be expressed (using B magnitude as an example):

$$\Delta B = 2.5 \log_{10}\left(1 + W_\lambda(1+z)\frac{R_B(\lambda)}{\int R_B(\lambda)d\lambda}\right), \tag{5}$$

where W_λ is the rest frame equivalent width in Å of the emission line, $\lambda = \lambda_{\rm rest}(1+z)$ is the observed wavelength of the line at redshift z, and R_B is the response of the B filter in Å^{-1} [43, 80]. Figure 24.6 shows the correction as a function of z for B, V magnitudes assuming equivalent widths for the strongest lines, Lyα, C IV, C III], Mg II, and H β, from Table 24.9 [81]. Differences between the emission line properties of radio-loud and radio-quiet quasars are generally negligible [82, 83], although significantly lower equivalent widths (by $\sim 30\%$) for C IV and Lyα in radio-quiet quasars have been reported [84].

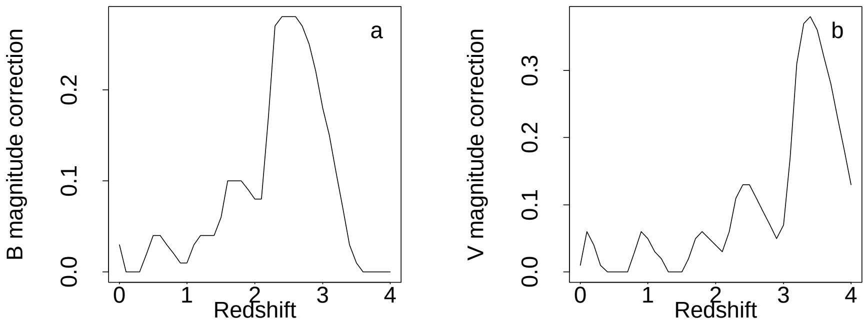

Figure 24.6. Correction to the (a) B magnitude and (b) V magnitude for the presence of emission lines as a function of redshift z using the equivalent widths given in Table 24.9.

Table 24.9. *Rest frame equivalent widths for emission lines in flat-spectrum, radio-loud quasars [1].*

Line	Wavelength (Å)	Equivalent width [W_λ (Å)]	$\sigma(W_\lambda)$	No.
[O III]	5007	32	28	30
Hβ	4861	47	25	26
[Ne III]	3869	5	2	21
[O II]	3727	8	6	23
[Ne V]	3426	6	6	23
Mg II	2798	27	15	113
C II]	2326	4	3	7
C III]	1909	17	12	96
He II	1640	4	3	7
C IV	1549	32	20	94
O IV]/Si IV	1400	6	3	14
O I	1304	4	3	14
Si II	1264	5	5	21
N V	1240	19	9	34
Lyα	1215	65	34	38
O VI	1034	15	13	12

Reference

1. Wilkes, B.J. 1986, MNRAS, **218**, 331

24.5.4 Photoionization Models

The emission lines from both regions are generally believed to arise predominantly in gas photoionized by the central continuum source. Figure 24.7 shows the relative strengths of the prominent emission lines as a function of the ionization parameter from a single zone. Excellent reviews are given in [66, 85], and line strengths for a wide range of cloud conditions are given in [86]. A standard, comprehensive photoionization computer code CLOUDY has been made generally available by anonymous ftp from Gary Ferland at the University of Kentucky http://www.pa.uky.edu/~gary/cloudy.

24.6 ABSORPTION LINES

The spectra of quasars contain a large number of absorption features due to gas clouds along the line of sight between us and the quasar. These features provide our only view of the distribution of matter out to high redshifts apart from the quasars themselves and thus their study is of primary importance to cosmology. Excellent reviews covering all aspects of absorption line research can be found in [87, 88]. Table 24.10 lists the main types of absorption system currently known.

Table 24.10. *Classes of absorption line systems seen in quasar spectra.*

System	log N_H (cm^{-2})	log($N_{\rm C\,IV}$) (cm^{-2})	b^a (km s^{-1})	Ionization	Comments
Lyα forest	13–16^b		20–30	$-3 \gtrsim$ LFN$^c \gtrsim -6$	
Metal–C IV	≥ 15.5	$\geq 13^b$	~100	$N_{\rm C\,IV} > N_{\rm C\,II}$	Intervening galaxies
Metal–Mg II	≥ 17.3		~100	$N_{\rm C\,IV} > N_{\rm C\,II}$	Intervening galaxies
Lyman limit (LLS)	≥ 17.3		~100	$N_{\rm C\,IV} > N_{\rm C\,II}$	~ Mg II systems
Damped Lyα	19–22		~100	$N_{\rm C\,IV} > N_{\rm C\,II}$	
Broad absorption line (BAL)	20–23	15–16	(5–10)$\times 10^3$	$N_{\rm C\,IV} > N_{\rm C\,II}$	Intrinsic?
21 cm	20.5–22		5–50	low	
Associated C IV, Mg II ^{d}	21–22	$\lesssim$ 100	$-5 \gtrsim$ LFN$^c \gtrsim -6$	$N_{\rm C\,VI} > N_{\rm C\,IV}$	Intrinsic?

Notes

^{a}Doppler width of H I systems: $b = \sqrt{2}\sigma$.
^{b}The lower limit of $N \sim 10^{13}$ cm^{-2} is a detection limit.
^{c}LFN = log(f$_{N_{\rm H\,I}}$), log of the fraction of H in the H I state.
^{d}Sometimes including an X-ray warm absorber [1].

Reference

1. Mathur, S., Wilkes, B.J., Elvis, M.S., & Fiore, F. 1994, ApJ, **434**, 493

24.6.1 Evolution and Distribution of Absorption Systems

The distribution of H I column densities is parametrized by $d\mathcal{N}/dN \propto N^{\beta}$, where $\mathcal{N}$ is the number of lines with column density N to $N + dN$ per unit redshift, z, and $\beta = 1.55 \pm 0.05$ for column density range: $12.6 <$ log N < 16.0 and $< z >= 3.7$ [89]. A complication to this distribution is the *inverse/proximity* effect whereby the density of lines decreases as the quasar redshift is approached [90, 91]. Table 24.11 gives evolution parameters for the various types of absorption line systems. Evolution with redshift is generally described in terms of a power

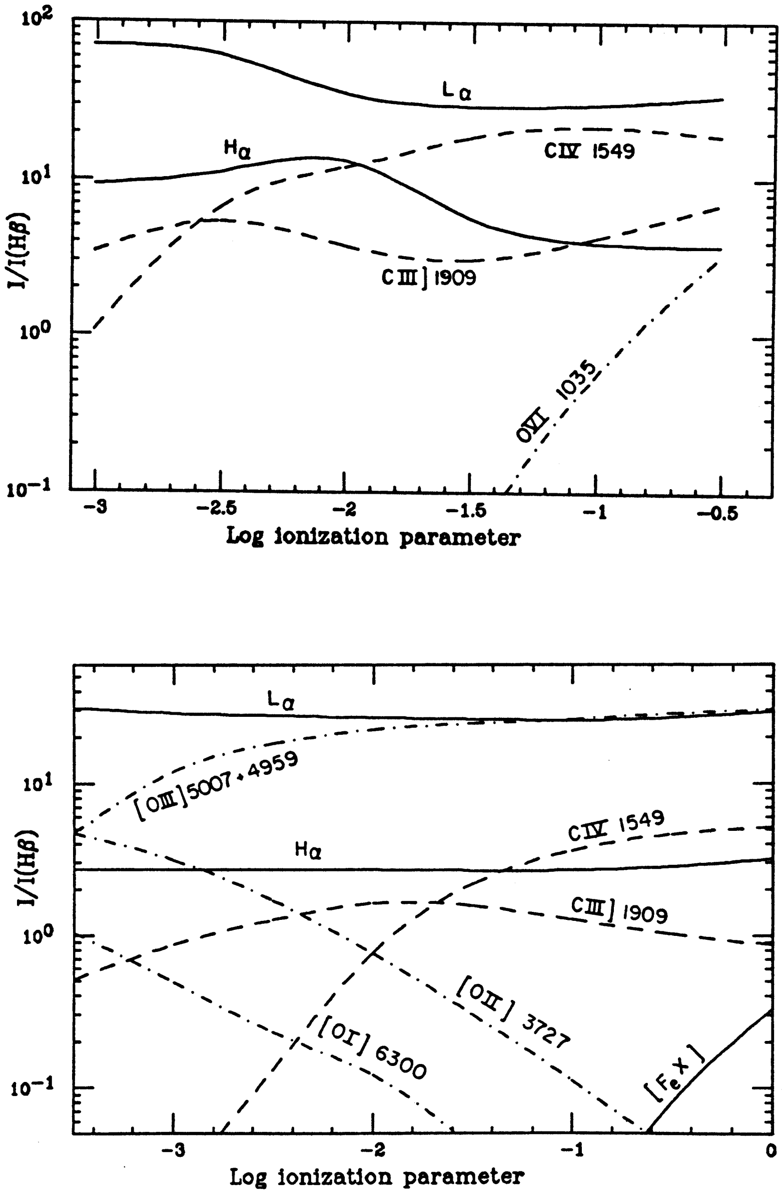

Figure 24.7. The strengths of the broad (upper) and narrow (lower) emission lines relative to Hβ as a function of the ionization parameter of the emitting gas in a single isolated BLR cloud with density 10^{10} cm^{-3} (from [66]).

law: $\mathcal{N}(z) \propto (1+z)^{\gamma}$. A value of γ between 0.5 and 1 is consistent with no evolution in the co-moving number density.

Table 24.11. *Evolution of the various absorption line systems.*

System	γ	z range	Reference
Lyα forest	~ 2.5	2.0–3.5	[1,2]
Lyα forest	0.58±0.50	z<1.3	[3]
C IV	−1.2±0.7	1.3–3.4	[4]
C IV	0.92±0.4	$\overline{z} = 0.3$	[5]
Mg II	0.78±0.42	0.2–2.2	[6]
LLS	1.50±0.39	0.3–4.1	[7]
Damped Lyα	1.3±0.5	2.8–4.4	[8]

References
1. Kim, T-S., Hu, E.M., Cowie, L.L. & Songaila, A. 1997 AJ, **114**, 1
2. Bechtold, J. 1994 ApJS, **91**, 1
3. Bahcall, J.N. *et al.* 1996 ApJ, **457**, 19
4. Sargent, W.L.W., Boksenberg, A., & Steidel, C.C. 1989, ApJS, **68**, 539
5. Bahcall, J.N., *et al.* 1993, ApJS, **87**, 1
6. Steidel, C.C., & Sargent, W.L.W. 1992, ApJS, **80**, 1
7. Stengler-Larrea, E.A. *et al.* 1995 ApJ, **444**, 64
8. Storrie-Lombardi, L.J., Irwin, M.J. & McMahon, R.G. 1996 MNRAS, **282**, 1330

24.7 SPECTRAL ENERGY DISTRIBUTIONS (SEDS)

Active galaxies are multiwavelength objects, emitting roughly equal energy in all wave bands throughout the electromagnetic spectrum. Complete observations can only be made using many different observing techniques, telescopes, satellites etc, Table 24.12 summarizes flux measurements typically made in each wave band. Transfer between various flux units is given in Chap. 9 and conversion of magnitude to flux is discussed in Chap. 15. Figures 24.8 and 24.9 show examples of radio-loud and radio-quiet quasar spectral energy distributions (SED) and the mean SED for low redshift quasars given by [39]. Table 24.13 lists the prominent features of quasar SEDs. Table 24.14 gives the bolometric corrections derived by Elvis *et al.* [39], their Table 21, based upon 43 SEDs in their sample.

Table 24.12. *Typical units for multiwavelength data.*

Wave band	Measurement	Units
Radio	Brightness temperature	kelvin (K)
	Power, S_ν	jansky (Jy)
mm	Power, S_ν	jansky (Jy)
IR	Magnitude	J, H, K, L, N, Q, See Chapter 15
	Spectrum: F_ν/F_λ	$\mathrm{erg\,cm^{-2}\,s^{-1}\,Hz^{-1}/erg\,cm^{-2}\,s^{-1}\,\AA^{-1}}$
Optical/UV	Magnitude	U, B, V, R, I
	Spectrum: F_ν/F_λ	$\mathrm{erg\,cm^{-2}\,s^{-1}\,Hz^{-1}/erg\,cm^{-2}\,s^{-1}\,\AA^{-1}}$
X-ray	Flux/flux density	$\mathrm{erg\,cm^{-2}\,s^{-1}}$ or $\mathrm{Jy/erg\,cm^{-2}\,s^{-1}\,Hz^{-1}}$
γ-ray	Photon flux	$\mathrm{photons\,cm^{-2}\,s^{-1}}$

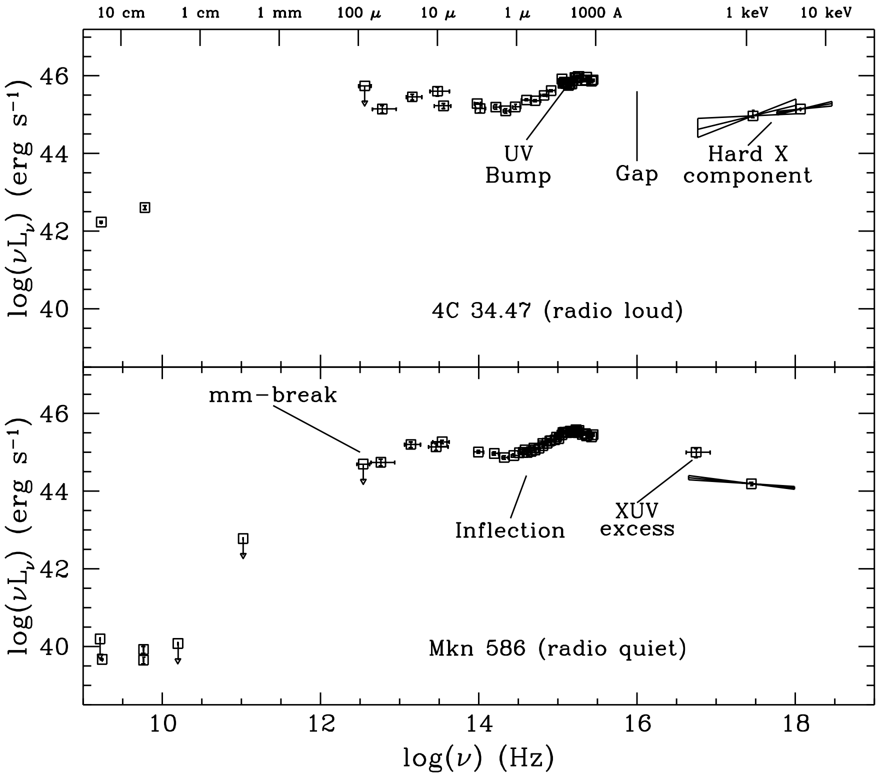

Figure 24.8. The radio–X-ray energy distribution of radio-loud quasar, 4C 34.47, and radio-quiet quasar, Mkn 586 (from [39], their Fig. 1).

Table 24.13. *Features and possible continuum energy generation mechanisms in the spectral energy distributions.*

Component	Mechanism	Reference
	All quasars	
OUV blue bump	Thermal: optically thick accretion disk	[1–3]
	optically-thin free-free	[4,5]
1-μm dip	> Dust sublimation temperature	[6]
IR bump	Thermal: cool + warm dust	[6]
	Nonthermal: synchrotron	[7]
X-ray	Seed spectrum, $\alpha_x \sim 1$	[8]
	Compton reflection	[9,10]
		[11]
	Thermal: accretion disk	[2,3]
	Radio-loud quasars	
Radio Core	Synchrotron, flat-spectrum, beamed	
	extends into IR–UV?	
Radio Lobes	Synchrotron, steep-spectrum, isotropic	
X-ray, radio-linked	Nonthermal: synchrotron self-Compton	[12]
	/pair production	[13]

Table 24.13. *(Continued.)*

Component	Mechanism	Reference
γ-ray	Non-thermal: synchrotron self-Compton	[14,15]
	Thermal: Comptonization	[16]

References
1. Sun, W.-S., & Malkan, M. 1989, ApJ, **346**, 68
2. Czerny, B., & Elvis, M. 1987, ApJ, **321**, 305
3. Laor, A. 1990, MNRAS, **246**, 369
4. Barvainis, R. 1993, ApJ, **413**, 513
5. Ferland, G.F., Korista, K.T., & Peterson, B.M. 1990, ApJ, **363**, L21
6. Sanders, D., Phinney, E.S., Neugebauer, G., Soifer, B.T., & Matthews, K. 1989, ApJ, **347**, 74
7. Carleton, N.P., Elvis, M., Fabbiano, G., Willner, S.P., Lawrence, A., & Ward, M., 1987, ApJ, **318**, 595
8. Haart, F., & Maraschi, L. 1993, ApJ, **413**, 507
9. Lightman, A.P., & White, T.R. 1988, ApJ, **335**, 57
10. Guilbert, P.W., & Rees, M.J. 1988, MNRAS, **233**, 475
11. Pounds, K.A., Nandra, K., Stewart, G.C., George, I.M., & Fabian, A.C. 1990, Nature, **344**, 132
12. Zamorani, G., *et al.* 1981, ApJ, **245**, 357
13. Lightman, A.P., & Zdziarski, A.A. 1987, ApJ, **319**, 643
14. Fichtel, C.E. *et al.* 1994, ApJS, **84**, 551
15. Bloom, S.D. & Marscher, A.P. 1996 ApJ, **461**, 657
16. Zdziarski, A.A., Johnson, W.N. & Magdziarz, P. 1996 MNRAS, **283**, 193

Table 24.14. *Bolometric corrections.*[a]

	Median	Mean, σ	Min.	Max.
$L_{\rm bol}/L_{2500\ \rm\AA}$	5.2	6.2±2.7	2.7	16.8
$L_{\rm bol}/L_{\rm B}$	10.4	11.5±4.4	5.1	25.1
$L_{\rm bol}/L_{\rm V}$	13.2	13.8±5.3	6.5	29.5
$L_{\rm bol}/L_{1.5\ \mu\rm m}$	24.3	25.4±9.1	8.7	41.8
$L_{\rm UVOIR}{}^b/L_{2500\rm\AA}$	3.5	4.1±2.2	1.4	12.8
$L_{\rm UVOIR}/L_{\rm B}$	7.0	7.5±3.5	4.2	22.7
$L_{\rm UVOIR}/L_{\rm V}$	8.2	9.0±4.1	4.7	23.0
$L_{\rm UVOIR}/L_{1.5\ \mu\rm m}$	15.6	16.1±5.6	8.1	29.5
$L_{\rm ion}{}^c/L_{\rm bol}$	0.32	0.32±0.13	0.07	0.68
$N_{\rm ion}R^d/L_{\rm bol}$	0.11	0.11±0.04	0.02	0.19
$L_{\rm ion}/N_{\rm ion}R$	2.8	3.0±0.8	1.7	5.0

Notes

[a]Bolometric correction factors for UV, visible (V), and IR monochrommatic luminosities [$\nu L(\nu)$ in the rest frame]. Errors in individual energy distributions have been ignored for the purposes of this table [1].

[b]$L_{\rm UVOIR}$: luminosity in the range 100–0.1 μm.

[c]$L_{\rm ion}$ = ionizing luminosity: 912 Å–10 keV.

[d]$N_{\rm ion}R$ = (number of ionizing photons) × 1 Ry.

Reference
1. Elvis, M., Wilkes, B.J., McDowell, J.C., Green, R.F., Bechtold, J., Willner, S.P., Cutri, R., Oey, M.S., & Polomski, E. 1994, ApJS, **95**, 1

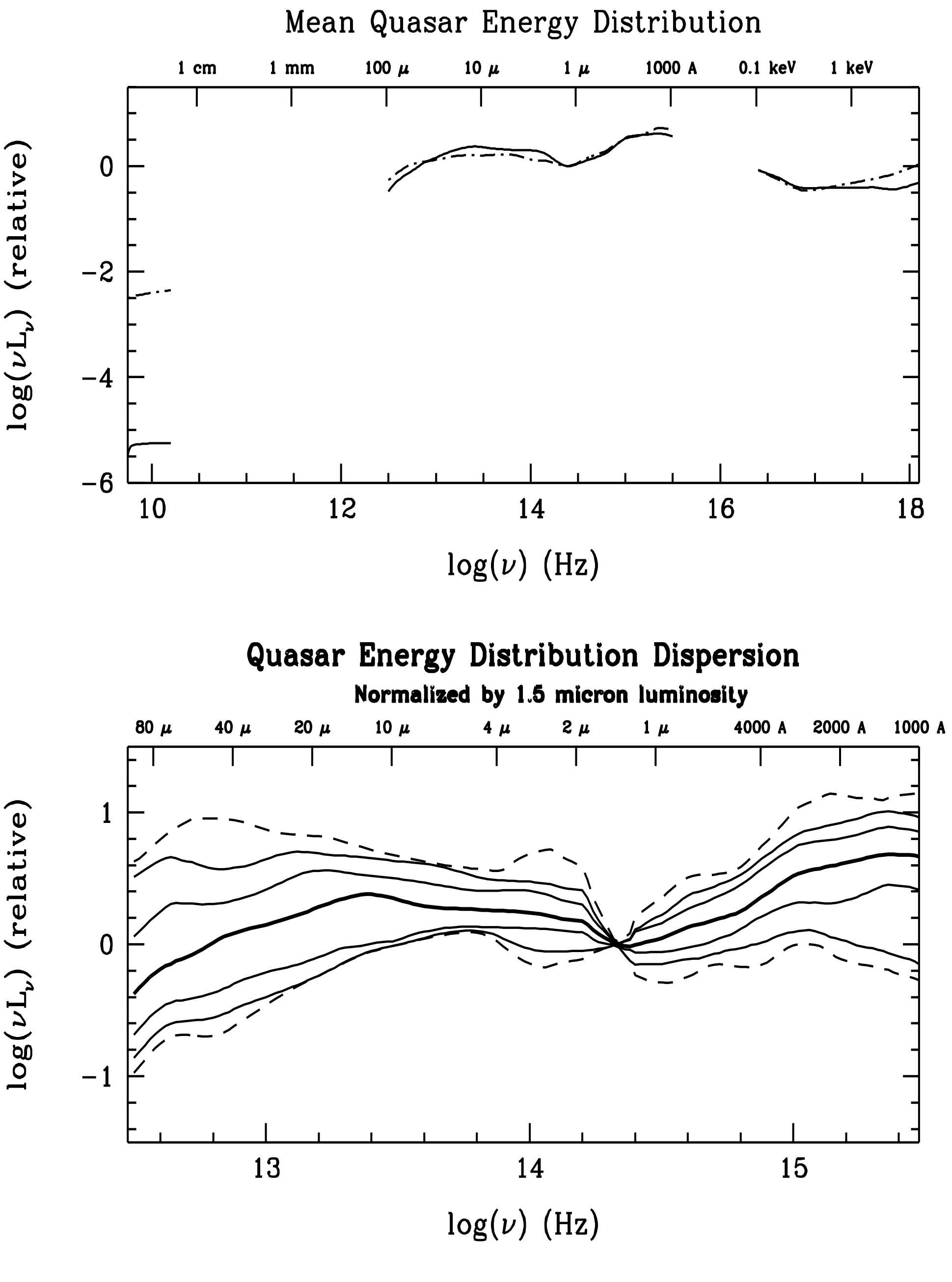

Figure 24.9. (top) The mean radio–X-ray spectral energy distribution of radio-loud (dashed line) and radio-quiet (solid line) quasars, and (bottom) the dispersion around the mean SED in the IR–UV region including 68, 90, and 100 percentile ranges (from [39], their Figure 11.)

24.8 LUMINOSITY FUNCTIONS AND THE SPACE DISTRIBUTION OF QUASARS

Figure 24.10 shows the optical surface density of quasars from the combined sample discussed in Hartwick & Schade [92], who also provide a comprehensive review of results in this area.

The observational luminosity function $\Phi(L,z)$ (=space density of quasars within a unit luminosity interval and in a limited redshift range) is generally determined using the $1/V_a$ statistic [92], their equation (3). Pure power law luminosity evolution gives acceptable fits to the data:

$$\Phi(L,z) = \frac{\Phi^*}{[L/L^*(z)]^\alpha + [L/L^*(z)]^\beta}.$$

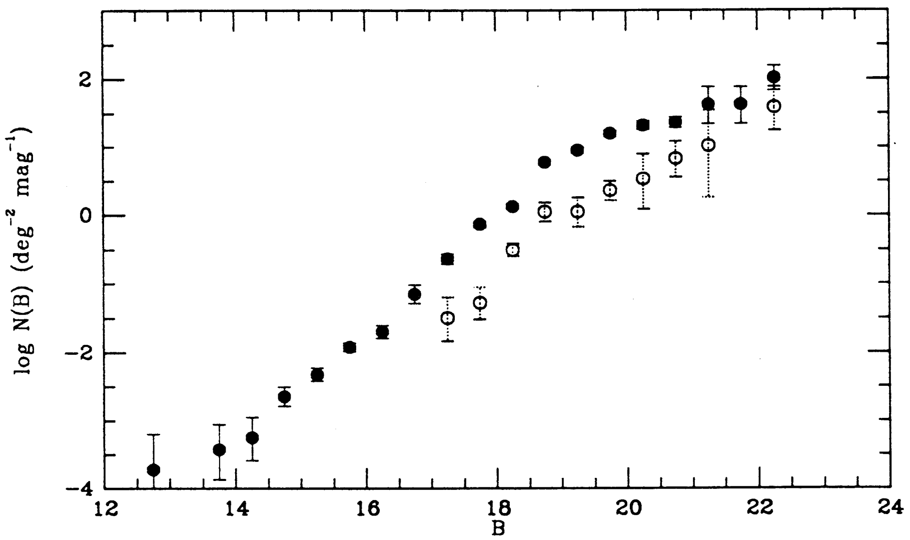

Figure 24.10. The optical surface density of quasars, from [92], solid symbols: 0<z<2.2; open symbols: 2.2<z<3.3.

Evolution is given by

$$L^*(z) = L^*(0)(1+z)^k \quad (z<2)$$

where L^* is the luminosity at the break between the two slopes α (L$\leq L^*$) and β (L$> L^*$). Table 24.15 lists values for these parameters and the relevant references.

Evolution in radio, optical, and X-ray bands slows/stops for $z \gtrsim 2$, although optical results from the LBQS [93] suggest that it continues at a slower rate, $k \sim$1.5 [94]. Figure 24.11 shows the luminosity function for the LBQS sample based on Table 4 of [95]. Note also that the presence of a range of slopes in the X-ray/optical continua could affect these results [96].

Table 24.15. *Parameters for pure, power law luminosity evolution in various spectral regions, $z<2$, for $q_o=0.0$.*

Param.	Optical 4400 Å	X-ray 2 keV	Radio (CDQs) 2.7 GHz	Units
α	3.6	3.3±0.2	2.9	
β	1.5	1.6±0.2	1.8	
$L^*(0)$	4.2×10^{29}	0.5×10^{44a}	2.3×10^{33}	$\mathrm{erg\,s^{-1}\,Hz^{-1}}$
Φ^*	5×10^{-7}	1×10^{-6}	2×10^{-9}	$\mathrm{mag.^{-1}\,Mpc^{-3}}$
k	3.50±0.05	$3.0^{+0.27}_{-0.40}$	~ 3	
z_{cut}	1.9	~1.6	~ 2	
Reference	[1]	[2]	[3]	

[a] erg s^{-1}, 0.3-3.5 keV

References
1. Boyle, B.J., Jones, L.R., & Shanks, T. 1991, MNRAS, **251**, 482
2. Jones, L.R. *et al.* 1997 MNRAS, **285**, 547
3. Dunlop, J.S., & Peacock, J.A. 1990, MNRAS, **247**, 19

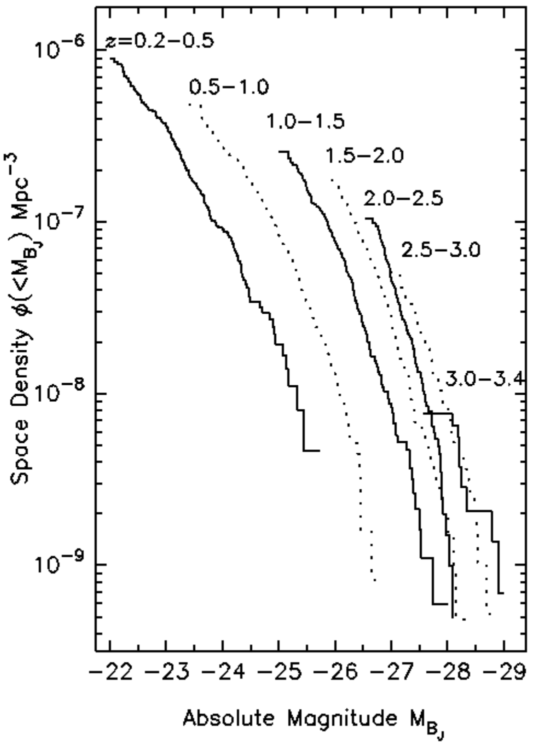

Figure 24.11. The cumulative space density of QSOs derived from the LBQS sample in seven redshift shells as labeled (figure of Table 4 from [95], courtesy of Paul Hewett).

24.9 BL LACS, HPQS, AND OVVS

The boundaries between these three classes are not always clear. OVVs are the strongly variable subset of HPQs, both of which have strong emission lines in their spectra at some/all epochs. Since in OVVs these lines sometimes disappear, more than one epoch of observations is required to distinguish between a BL Lac and an OVV, for this reason the two classes are often referred to jointly as blazars. However it should be noted that there are observational differences between OVVs and BL Lacs that should discourage such unification [97–100]. BL Lacs, due to their lack of emission lines, are most efficiently found in radio or X-ray surveys resulting in their division into two sub-categories: RBL, radio-selected BL Lac (or LBL, low-frequency peaked SED); and XBL, X-ray selected BL Lac (or HBL, high-frequency peaked SED). Discussion continues as to whether or not these are distinct classes.

Table 24.16 lists salient parameters for these objects. A conference proceedings dealing with all aspects of BL Lac Objects and OVVs is [101].

Table 24.16. *General characteristics of highly polarized AGN.*

Property	BL Lac	HPQ	OVV	Reference
Optical morphology	Point Source	Point Source	Point Source	
Continuum	Smooth $\lambda < 10\ \mu$m	Weak BB^a	Weak BB^a	
Emission lines	No	Yes	Yes	
Parent population	FRI RGs	FRII RGs	FRII RGs	[1]
$P_{\rm opt}$	3–40%	3–20%	3–20%	[2,3]
$T_{\rm var}$	Days	Days–years	Days	
Δm	1–5	0.5–5	1–5	[2,4]
μ (ang'r vel'y)	0.1–0.8	0.05–2.7	0.05–2.7	[5]
$\beta_{\rm app}$	2–4	1–18.5	1–18.5	[5]

Note
^{a}BB = optical/UV blue bump.

References
1. Padovani, P., & Urry, C.M. 1990, ApJ, **356**, 75
2. Angel, J.R.P., & Stockman, H.S. 1980, ANRAA, **18**, 321
3. Stockman, H.S., Moore, R.L., & Angel, J.R.P. 1984, ApJ, **279**, 485
4. Moore, R.L., & Stockman, H.S. 1984, ApJ, **279**, 465
5. Zensus, J.A. 1989, in BL Lac Objects, Lecture Notes in Physics 334, eds. L. Maraschi, T. Maccacaro, and M.-H. Ulrich (Springer, Berlin), p. 3

24.10 LOW-LUMINOSITY ACTIVE GALACTIC NUCLEI (LLAGN)

These objects have lower luminosity than quasars; $M > -23$ and $z \lesssim 0.1$. A comprehensive review can be found in [102]. Table 24.17 lists values of commonly used parameters for each class of LLAGN. Figure 24.2 shows the line ratio properties in graphical form. Recent results have shown that weak AGN are present in $\sim$ 20% of all AGN and $\sim$ 10% of all luminous galaxies [33].

Table 24.17. *Typical values for common parameters.*

	Sy1/BLRG	Sy2/NLRG	LINER	Starburst	Reference
Host galaxy^a	Sp/E	Sp/E	Sp	Sp	[1]
FWHM^b (km s^{-1})	10^3–10^4	10^2–10^3	200–400		
log ($\mathcal{M}_{BH}/\mathcal{M}_\odot$)	7.5–9.0				[2]
log U	-2^c	-3	-3.5		[3]
α_x(0.1–3.5 keV)^d	0.5–2/0–1^e	0.5–2/0–1^e	0.5–2^e		[4]
α_x(2–10 keV)	0.7–1^e	~ 0.4			[5,6]
l	0 to >200	0 to >200			[7,8]
[O III]/Hβ	1.5–3	3–20	0.1–1.5	0.03–8	[3,9,10]
[N II]/Hα		> 0.5	> 0.5	< 0.5	[3,9]
[O I]/Hα		> 0.08	> 0.08	< 0.08	[3,9]
[S II]/Hα		> 0.4	> 0.4	< 0.4	[3,9]
[O II]/[O III]	≤ 0.5	0.1–1	1–10	> 1	[3]
[O I]/[O III]			>0.33		[11]

Notes

^{a}Most likely morphology of host galaxy: Sp = spiral, E = elliptical.
^{b}The FWHM increases with the critical density of the forbidden line [12].
^{c}Narrow-line region (log $U \sim -1$ for the BLR).
^{d}90% confidence range.
^{e}There is marginal evidence that Sy2, NLRGs, and LINERs have flatter X-ray slopes than Sy1/BLRGs.

References

1. McLeod, K.K., & Rieke, G.H. 1994, ApJ, **420**, 58
2. Sun, W.-S., & Malkan, M. 1989, ApJ, **346**, 68
3. Netzer, H. 1990, in Active Galactic Nuclei, eds. T. Courvoisier & M. Mayer (Springer, Berlin), p. 57
4. Kruper, J.S., Urry, C.M., & Canizares, C.R. 1990, ApJS, **74**, 347
5. Turner, T.J., & Pounds, K.A. 1989, MNRAS, **240**, 833
6. Awaki, H., *et al.* 1991, PASJ, **43**, 195
7. Done, C., & Fabian, A.C. 1990, MNRAS, **240**, 81
8. Lightman, A.P., & Zdziarski, A.A. 1987, ApJ, **319**, 643
9. Osterbrock, D. 1989, Astrophysics of Gaseous Nebulae and Active Galactic Nuclei (University Science Books, Mill Valley)
10. Shuder, J.M., & Osterbrock, D.E. 1981 ApJ, **250**, 55
11. Heckman, T.M. 1980 A&A, **87**, 152
12. Filippenko, A.V. 1985, ApJ, **289**, 475

24.11 AGN ENVIRONMENTS

Low-redshift quasars and AGN are known to be embedded in galaxies. Relatively large samples (with > 20 objects) of nearby quasars have now been studied with ground-based charge-coupled devices (CCDs) [103–108] and infrared arrays [109–112]. and with the *Hubble* Space Telescope [113–116].

Many of the closest quasars ($z \lesssim 0.1$), which are in general radio-quiet and low-luminosity objects, live in spiral hosts, although there is a strong bias against edge-on spirals [103, 111]. Elliptical hosts have also been reported for several radio-quiet quasars [113]. Radio-loud quasar hosts are generally thought to be elliptical though fits to host-galaxy luminosity profiles for these and other high-luminosity quasars are ambiguous. The most luminous quasars are only found in luminous galaxies ($\sim L^*$, [107, 112]). Close companions and/or complex morphology (implying recent interactions) are common [113, 115, 117]. A recent conference proceedings providing a comprehensive review of the subject is [118].

For the few BL Lac objects with data available, the hosts are generally elliptical [119], although a few are spiral [120].

REFERENCES

1. Schmidt, M. 1963, Nature, **197**, 1040
2. Hazard, C., Mackay, M.B., & Shimmins A.J. 1963, Nature **197**, 1037
3. Greenstein, J.L., & Schmidt, M. 1964, ApJ, **140**, 1
4. Sandage, A.R. 1965 ApJ, **141**, 1560
5. Seyfert, C.K. 1943, ApJ, **97**, 28
6. Peterson, B.M. 1997, An Introduction to Active Galactic Nuclei (Cambridge University Press, Cambridge)
7. Stocke, J.S., Morris, S.L., Gioia, I.M., Maccacaro, T., Schild, R., Wolter, A., Fleming, T.A., & Henry, J.P. 1991, ApJS, **76**, 813
8. Veilleux, S., & Osterbrock, D.E. 1987, ApJS, **63**, 295
9. Evans, I.N., & Dopita, M.A. 1985, ApJS, **58**, 125
10. McCall, M.L., Rybski, P.M., & Shields, G.A. 1985, ApJS, **57**, 1
11. Green, P.J., Anderson, S.F., & Ward, M.J. 1992, MNRAS, **254**, 30
12. Wilkes, B.J. 1984, MNRAS, **207**, 73
13. Kallman, T.R., Wilkes, B.J., Krolik, J.H., & Green, R.F. 1993, ApJ, **403**, 45
14. Weymann, R.J., Morris, S.L., Foltz, C. B., & Hewett, P.C. 1991, ApJ, **373**, 23
15. Allen, R.G., Smith, P.A., Angel, J.R.P., Miller, B.W., Anderson, S.F., & Margon, B. 1993, ApJ, **403**, 610
16. Peterson, B.M. *et al.* 1992, ApJ, **392**, 470
17. Hewitt, A., & Burbidge, G. 1993, ApJS, **87**, 451
18. Véron-Cetty, M.-P., & Veron, P. 1993, ESO Scientific Report No. 13
19. Padovani, P. & Giommi, P. 1995 MNRAS, **277**, 1477
20. Hewitt, A., & Burbidge, G. 1991, ApJS, **75**, 297
21. Junkkarinen, V., Hewitt, A., & Burbidge, G. 1991, ApJS, **77**, 203
22. MacAlpine, G.M., Lewis, D.W., & Smith, S.B. 1977, ApJS, **35**, 203
23. Wilkes, B.J., Wright, A.E., Peterson, B.A., & Jauncey, D.L. 1983, Astron. Soc. Aust. Conf. Proc. **5**, 2
24. Anderson, S.F., & Margon, B. 1987 ApJ, **314**, 111
25. Baldwin, J.A., Wampler, E.J., & Gaskell, C.M. 1989, ApJ, **338**, 630
26. Keel, W.C. 1983, ApJS, **52**, 229
27. Wolfe, A.M., Turnshek, D.A., Smith, H.E., & Cohen, R.D. 1986, ApJS, **61**, 249
28. Irwin, M., McMahon, R.G., & Hazard, C. 1991, ASP Conference Series **21**, The Space Distribution of Quasars, ed. D. Crampton, p. 117
29. Schneider, D.P., Schmidt, M. & Gunn, J.E. 1994 AJ, **107**, 1245
30. Kinney, A.L., Bohlin, R.C., Blades, J.C., & York, D.G. 1991, ApJS, **75**, 645
31. Lanzetta, K.M., Turnshek, D.A., & Sandoval, J. 1993, ApJS, **84**, 109
32. Kinney, A.L., Bohlin, R.C., Calzetti, D., Panagia, N., & Wyse, R.F.G. 1993, ApJS, **86**, 5
33. Ho, L.C., Filippenko, A.V.,Sargent, W.L.W. & Peng, C.Y. 1997 ApJS, **112**, 391
34. Low, F.J., Cutri, R.M., Huchra, J.P. & Kleinmann, S.G., 1988, ApJL, **327**, 41
35. Rush, B., Malkan, M. & Spinoglio, L. 1993 ApJS, **89**, 1
36. Kleinmann, S. G. *et al.* 1994 A&SS, **217**, 11
37. Sanders, D., Phinney, E.S., Neugebauer, G., Soifer, B.T., & Matthews, K. 1989, ApJ, **347**, 29
38. Impey, C.D., & Neugebauer, G. 1988, AJ, **95**, 307
39. Elvis, M., Wilkes, B.J., McDowell, J.C., Green, R.F., Bechtold, J., Willner, S.P., Oey, M.S., Polomski, E. & Cutri, R. 1994, ApJS, **95**, 1
40. Maccacaro, T., Della Ceca, R., Gioia, I.M., Morris, S.L., Stocke, J.T., & Wolter, A. 1991, ApJ, **374**, 117
41. Piccinotti, G., Mushotzky, R.F., Boldt, E.A., Holt, S.S., Marshall, F.E., Serlemitsos, P.J., & Shafer, R.A. 1982, ApJ, **253**, 485
42. Schwartz, D.A. *et al.* 1989, BL Lac Objects, in Lecture Notes in Physics **334**, eds. L. Maraschi, T. Maccacaro, & M.-H. Ulrich (Springer, Berlin), p. 209
43. Wilkes, B.J., Tananbaum, H., Worrall, D.M., Avni, Y., Oey, M.S., & Flanagan, J. 1994, ApJS, **92**, 53
44. Elvis, M., Plummer, D., Schachter, J., & Fabbiano, G. 1992, ApJ, **80**, 257
45. Giommi, P. *et al.* 1989, BL Lac Objects, in Lecture Notes in Physics **334**, eds. L. Maraschi, T. Maccacaro, & M-H. Ulrich (Springer, Berlin), p. 231
46. Voges, W. *et al.* 1996, IAUC, 6420
47. Boyle, B.J., Griffiths, R.E., Shanks, T., Stewart, G.C. & Georgantopolous, I. 1993, MNRAS, **260**, 49
48. Green, P.J., Schartel, N., Anderson, S.F., Hewett, P.C., Foltz, C.B., Fink, H.H., Brinkmann, W., Trümper, J., & Margon, B. 1995, ApJ, **450**, 51

49. Boyle, B.J., Wilkes, B.J., & Elvis, M. 1997, MNRAS, **285**, 511
50. Puchnarewicz, E.M., Mason, K.O., Romero-Colmenero, E., Carrera, F.J., Hasinger, G., McMahon, R., Mittaz, J.P.D., Page, M.F., & Carballo, R. 1996, MNRAS, **281**, 1243
51. Singh, K.P., Barrett, P., White, N.E., Giommi, P., & Angelini, L. 1995, ApJ, **455**, 456
52. Fichtel, C.E., *et al.* 1994, ApJS, **94**, 551
53. Masson, C.R., & Wall, J.V. 1977, MNRAS, **180**, 193
54. Kellerman, K.I., Sramek, R., Schmidt, M., Shaffer, D.B., & Green, R.F. 1989, AJ, **98**, 1195
55. Kuhr, H., Pauliny-Toth, I.I.K., Witzel, A., & Schmidt, J. 1981a, AJ, **86**, 854
56. Condon, J. J., Cotton, W. D., Greisen, E. W., Yin, Q. F., Perley, R. A., Taylor, G. B., & Broderick, J. J. 1998 AJ, **115**, 1693
57. Gregg, M.D., Becker, R.H., White, R.L., Helfand, D.J., McMahon, R. G. & Hook, I.M. 1996 AJ, **112**, 407
58. Tananbaum, H. *et al.* 1979, ApJ, **234**, L9
59. Zamorani, G. *et al.* 1981, ApJ, **245**, 357
60. Impey, C.D., & Tapia, S. 1990, ApJ, **354**, 124
61. Wilkes, B.J., & Elvis, M. 1987, ApJ, **323**, 243
62. Shastri, P., Wilkes, B.J., Elvis, M., & McDowell, J.C. 1993, ApJ, **410**, 29
63. Orr, M.J.L., & Browne, I.W.A. 1982, MNRAS, **200**, 1067
64. Sziemiginowska, A., Kuhn, O., Elvis, M., Fiore, F., McDowell, J., & Wilkes, B.J. 1995, ApJ, **454**, 77
65. Guilbert, P.W., Fabian, A.C., & Rees, M.J. 1983, MNRAS, **205**, 593
66. Netzer, H. 1990, in Active Galactic Nuclei, eds. T.J-L. Courvoisier & M. Mayor (Springer, Berlin), p. 57
67. Baldwin, J.A., Phillips, M.M., & Terlevich, R. 1981, PASP, **93**, 5
68. Emission Lines in Active Galaxies: New Methods and Techniques, 1997 eds. B.M. Peterson, F.-Z. Cheng and A.S. Wilson (San Francisco: Astronomical Society of the Pacific)
69. Boroson, T., & Green, R.F. 1992, ApJS, **80**, 109
70. Vestergaard, M. & Wilkes, B.J. 1998 ApJ, *submitted*
71. Nandra, K., George, I.M., Mushotzky, R.F., Turner, T.J., & Yaqoob, T 1997, ApJ, **477**, 602
72. Matt, G., Fabian, A.C. & Ross, R.R. 1996 MNRAS, **278**, 1111
73. Mushotzky, R.F., Done, C. & Pounds, K.A. 1993, ANRAA, **31**, 717
74. Netzer, H. 1997 in Emission Lines in Active Galaxies: New Methods and Techniques, eds. B.M. Peterson, F.-Z. Cheng and A.S. Wilson (San Francisco: Astronomical Society of the Pacific), p.20
75. Francis, P.J., Hewett, P.C., Foltz, C.B., Chaffee, F.H., Weymann, R.J., & Morris, S.L. 1991, ApJ, **373**, 465
76. Baldwin, J.A. 1997 in Emission Lines in Active Galaxies: New Methods and Techniques, eds. B.M. Peterson, F.-Z. Cheng and A.S. Wilson (San Francisco: Astronomical Society of the Pacific), p.80
77. Korista, K.T. *et al.* 1995 ApJ, **97**, 285
78. ASP Conference Series Volume 69, on Reverberation Mapping of the Broad-Line Region in Active Galactic Nuclei 1994, eds. P.M. Gondhalekar, K. Horne, and B.M. Peterson
79. Ulrich, M-H., Maraschi, L. & Urry, C.M. 1997 ANRAA **35**, 445
80. Marshall, H.M. 1983, Ph.D. thesis, Harvard University
81. Wilkes, B.J. 1986, MNRAS, **218**, 331
82. Corbin, M.R. 1992, ApJ, **391**, 577
83. Steidel, C.C., & Sargent, W.L.W. 1991, ApJ, **382**, 433
84. Francis, P.J., Hooper, E.J., & Impey, C.D. 1993, AJ, **106**, 417
85. Ferland, G.F., & Shields, G.A. 1985, in Astrophysics of Active Galaxies and Quasars, ed. J. Miller (University Science Books, Mill Valley), p. 157
86. Baldwin, J. *et al.* 1995, ApJ, **455**, L119
87. Blades, C., Turnshek, D., & Norman, C.A., eds. 1988, QSO Absorption Lines: Probing the Universe (Cambridge University Press, Cambridge)
88. Meylan, G. ed. 1995, QSO Absorption Lines: Proceedings of ESO Workshop (Springer, Berlin; New York)
89. Lu, L, Sargent, W.L.W, Woble, D.S. & Takada-Hidai, M. 1996 ApJ, **472**, 509
90. Murdoch, H.S., Hunstead, R.W., Pettini, M. & Blades, J.C. 1986, ApJ, **309**, 19
91. Weymann, R.J., Carswell, R.F., & Smith, M.G. 1981, ANRAA, **19**, 41
92. Hartwick, F.D.A., & Schade, D. 1990, ANRAA, **28**, 437
93. Morris, S.L., Weymann, R.J., Anderson, S.F., Hewett, P.C., Foltz, C.B., Chaffee, F.H., Francis, P.J., & MacAlpine, G.M. 1991, AJ, **102**, 1627
94. Hewett, P.C., Foltz, C.B., & Chaffee, F.H. 1993, ApJ, **406**, L43
95. Hewett, P.C., Foltz, C.B., & Chaffee, F.H. 1995, AJ, **109**, 1498
96. Francis, P.J., 1993, ApJ, **407**, 519
97. Worrall, D.M., & Wilkes, B.J. 1990, ApJ, **360**, 396
98. Smith, P.S., Balonek, T.J., Elston, R., & Heckert, T.A. 1987, ApJS, **64**, 459
99. Browne, I.W.A. 1989, BL Lac Objects, in Lecture Notes in Physics **334**, eds. L. Maraschi, T. Maccacaro,

& M-H. Ulrich (Springer, Berlin), p. 401
100. Miller, J.S. 1989, in BL Lac Objects, Lecture Notes in Physics **334**, eds. L. Maraschi, T. Maccacaro, & M-H. Ulrich (Springer, Berlin), p. 395
101. Maraschi, L., Maccacaro, T., & Ulrich, M-H. 1989, BL Lac Objects, Lecture Notes in Physics **334** (Springer, Berlin)
102. Osterbrock, D.E. 1993, ApJ, **404**, 551
103. Malkan, M.A., Margon, B., & Chanan, G.A. 1984, ApJ, **280**, 66
104. Malkan, M.A. 1984, ApJ, **287**, 555
105. Hutchings, J.B., 1987, ApJ, **320**, 122
106. Hutchings, J.B., Janson, T., & Neff, S.G. 1989, ApJ, **342**, 660
107. Véron-Cetty, M.-P., & Woltjer, L. 1990, A&A, **236**, 69
108. Green, R.F., & Yee, H.K.C. 1984, ApJS, **54**, 495
109. Dunlop, J.S., Taylor, G.L., Hughes, D.H., & Robson, E.I. 1993 MNRAS, **264**, 455
110. Taylor, G.L., Dunlop, J.S., Hughes, D.H., & Robson, E.I. 1996 MNRAS, **283**, 930
111. McLeod, K.K., & Rieke, G.H. 1994a, ApJ, **420**, 58
112. McLeod, K.K., & Rieke, G.H. 1994b, ApJ, **431**, 137
113. Bahcall, J.A., Kirhakos, S., & Schneider, D.P. 1995, ApJ, **450**, 486
114. Hutchings, J.B. & Morris, S.C. 1995, AJ, **109**, 1541
115. Hutchings, J.B. & Neff, S.G. 1992, AJ, **104**, 1
116. Hooper, E.J., Impey, C.D. & Foltz, C.B. 1997 ApJ, **480**, L95
117. Boyce, P.J., Disney, M.J., Blades, J.C., Boksenberg, A., Crane, P., Deharveng, J.M., Macchetto F.D., Mackay, C.D. & Sparks, W.B. 1996 ApJ, **473**, 760
118. Clements, D. & Perez-Fournon, I., eds. 1997, ESO Astrophysics Symposia: Quasar Hosts (Springer-Verlag, Berlin Heidelberg)
119. Ulrich, M-H. 1989, BL Lac Objects, Lecture Notes in Physics **334**, eds. L. Maraschi, T. Maccacaro, and M.-H. Ulrich (Springer, Berlin)
120. Abraham, R.G., Crawford, C.S. & McHardy, I.M. 1991, MNRAS, **252**, 482 **334**, 597